Sixth International Symposium on Turbulence and Shear Flow Phenomena
Seoul, Korea, 22-24 June 2009

EDDY SIMULATION OF TURBULENT MIXING OVER TURBINE BLADE TRAILING EDGE BREAKOUT

Jongwook Joo
Department of Aerospace Engineering,
Iowa State University
Howe Hall, Ames, Iowa, 50011, USA
jwjoo@iastate.edu

Paul A. Durbin
Department of Aerospace Engineering,
Iowa State University
Howe Hall, Ames, Iowa, 50011, USA
durbin@iastate.edu

ABSTRACT

The cause of over prediction of cooling efficiency by unsteady, Reynolds averaged simulations of turbine blade trailing edge cooling flow is investigated. It is due to deficiency in the level of unsteady, coherent energy very near to the wall. Farther from the wall, Reynolds averaged simulation produces the correct level of mixing. Eddy simulations of the instantaneous, turbulent eddying produce close agreement to data on film effectiveness. In particular, they reproduce the reduction of cooling effectiveness toward the trailing edge that has been seen in experiments. The Scale Adaptive Simulation model of Menter and Egorov (2005a) is invoked for the eddy simulations.

MOTIVATION

Trailing edges of turbine blades are susceptible to excessive heating by hot ambient gasses and difficult to cool. In the standard cooling strategy, the rear portion of the blade has an opening on the pressure side through which gas that has transited internal passages exits. After exiting it creates a jet tangential to the surface. It is expected to form a cooling shield over the surface.

The terminology used herein is as follows (see figure 1). The opening is referred to as a *break out*. The exposed portion of the wall jet is bounded by raised portions of the blade called *lands*. The upper edge of the nozzle is called the *nozzle lip*.

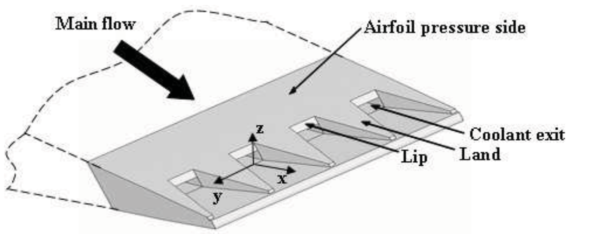

Figure 1: Trailing edge cooling slots at pressure side breakout.

The adiabatic *cooling effectiveness* is the ratio of hot gas temperature minus surface temperature to hot gas minus coolant temperature:

$$\eta_{ad} = (T_g - T_s)/(T_g - T_c)$$

Unfortunately, laboratory tests show that the film cooling effectiveness decreases to about 0.5 near the trailing edge at typical blowing ratios (blowing ratio is the ratio of bulk mass flow from the slot to that in the free-stream). This low performance of film cooling implies that some kind of mixing phenomena between the co-flowing hot gas and the cooling air streams is occurring. Since its source is not well understood, it will be called *anomalous mixing*.

Most numerical studies of the trailing edge configuration have employed Reynolds averaged (RANS) models (Menter and Egorov, 2005a; Holloway et al., 2002a; Holloway et al., 2002b; Medic and Durbin, 2005). Unsteady RANS shows that coherent vortex shedding from the nozzle lip plays a critical role in the flow around the break out.

Unfortunately, in all of these studies the natural unsteadiness was unable to reproduce the drop in effectiveness seen in laboratory experiments; in the case computed by Medic and Durbin (2005). and by Holloway et al. (2002b) the observed effectiveness was 0.5, while the computed effectiveness was 0.9. An unknown process seemed to enhance mixing beyond what could be explained by vortex shedding alone.

Further RANS simulations (Medic and Durbin, 2005) in which the cooling flow was pulsed periodically were able to reproduce the observed drop of effectiveness. The forcing caused the shed vortices to develop into vortex loops, which enhanced mixing and decreased η_{ad}. These simulations suggest a possible cause of the strong mixing present in real trailing edge breakouts. Is there any reason for the coherent vortex loops to form more naturally?

This and other questions can be answered by simulating the turbulent, eddying flow downstream of the breakout. Eddy simulation promises detailed information which can reveal the complex, and poorly understood, mixing mechanisms that occur in this flow.

Menter and Egorov (2005a) presented a form of eddy simulation which they called scale-adaptive simulation (SAS). Functionally, it involves adding a term that constrains the level of eddy viscosity provided by the RANS model, thereby permitting chaotic eddying to occur.

We use 'eddy simulation' as a general term to refer to computations in which the chaotic state of turbulence is resolved in contrast to RANS computations. SAS grew out of detached *eddy simulation*. The eddying region is regarded as a large *eddy simulation* region. As will be seen, our simulation turns out to be similar to LES in the breakout region. Rather than describe this as a qualified version of either detached or large eddy simulation, it is preferable to adopt the generic term 'eddy simulation'.

NUMERICAL METHODS AND MODELS

The simulations made use of the SuMB computational fluid dynamics code as described in Van der Weide et al. (2006). This is a multi-block, structured grid code. It solves the fully compressible, Reynolds averaged Navier-Stokes equations, discretized into finite volumes. Solution variables are collocated at cell centers. Time accuracy is achieved by dual time-stepping. The true time-step is discretized by second order, backward Euler differencing. Each true time-step is sub-integrated in pseudo-time by the 5 stage, Runge-Kutta scheme of Jameson (1985). Convergence is accelerated by multi-grid iterations. The Runge-Kutta integrations function as a smoother on the successively coarser grids.

A number of modifications to the numerical discretization and time advancement methods were effected for the present application. These were required in order to obtain the accuracy and stability needed for eddy simulation.

Scale adaptive simulation

The SST, RANS model (Menter, 1992) is a variant of the $k-\omega$ model. The scale adaptive SST model is the RANS model with an extra term in the ω equation. In SAS, the adaptive scale is provided by the von Karman length (Menter and Egorov, 2005b)

$$L_{vk} = \max\left[\frac{\kappa|\boldsymbol{S}|}{|\nabla^2\boldsymbol{U}|}, \frac{0.358C_\mu\Delta}{\beta - C_\mu\alpha}\right] \qquad (1)$$

where $\kappa = 0.41$, $C_\mu = 0.09$, $\beta = 3/40$ in the $k-\omega$ model and

$$|\boldsymbol{S}|^2 = 2S_{ij}S_{ji} \quad \text{with} \quad 2S_{ij} = \partial_i U_j + \partial_j U_i \qquad (2)$$

If L_{vk} were used in an eddy viscosity transport model, assuming that destruction and production were in balance would give

$$\nu_T \sim L_{vk}^2|\boldsymbol{S}| \qquad (3)$$

Thus L_{vk} can be understood to be a bit like a mixing length.

A limiter on L_{vk} prevents the eddy viscosity from dropping below the level of the Smagorinsky subgrid model in order to ensure that the model dissipates small scales

The formulation of the extra term in the ω equation is described in Menter and Egorov (2005b).

Treatment of convection

Eddy simulation requires convection schemes with low dissipation. The native discretizations in SuMB are unsatisfactory for present purposes. A skew symmetric convective form was found to be stable and accurate. The rationales given in the literature for this form are consistency with kinetic energy conservation, via the discrete product rule, and reduction in aliasing error (Blaisdell et al., 1996).

Transported scalars are especially prone to numerical oscillations. It has become common practice in eddy simulation to invoke some degree of upwinding. The second order, upwind method of Barth and Jespersen (1989) was selected. It invokes a limiter to minimize numerical diffusion; thus, on a smooth field it relaxes to second order central differencing.

Implicit Compact Filtering

A weak numerical instability was observed as simulations proceeded. As it was of high spatial frequency, a low pass filter was applied periodically to suppress it. A compact, Padé type of formulation was used. Several families of filtering schemes were discussed in (Lele, 1992). 4th order accuracy filter which solves tri-diagonal matrix was chosen for this study. The compact filter was applied for all field variables once every 47 time steps to remove grid-wise oscillation.

Inflow conditions

It proved necessary to include turbulent eddies at the inflow in order to stimulate turbulent motion in the separation region. To this end, inflow data were generated by a separate large eddy simulation of a turbulent boundary — the LES code was provided by Kang and Choi (2002). The rescaling and recycling technique of Lund et al. (1998) was used to create a fully developed boundary layer.

While the LES simulation provides a full velocity field, quantities such as k and ω also are needed for the SST-SAS model. In the SAS mode, k and ϵ can be understood as subgrid scale residual kinetic energy and dissipation. Assuming that the LES field resolves almost all turbulent kinetic energy, a box filter was applied over the field. The filter width was small enough to preserve most of the energy. The residual kinetic energy was defined as

$$k = \frac{1}{2}U_iU_i - \frac{1}{2}\hat{U}_i\hat{U}_i$$

ϵ was estimated from subgrid scale dissipation as

$$\epsilon \approx 2\nu_{T,SGS}S_{ij}S_{ij}$$

Finally ω was evaluated as $\omega = \epsilon/(0.09k)$.

FLOW CONFIGURATION

The computational domain is portrayed at the left of figure 2. The coolant inflow data are provided by a large eddy simulation of fully developed channel flow. The bulk velocity is unity by the present non-dimensionalization. The lateral boundary conditions are periodic.

The eddy simulation was preceded by a RANS computation on the domain shown at the top of figure 3. This contains a whole blade in a domain that was designed to emulate the pressure field of a turbine stage (this particular configuration is being studied in experiments by Chen et al. (2007) at Stanford University). SuMB was used for both RANS and eddy simulations. The RANS simulation provided a mean flow at the inlet to the eddy simulation. This procedure is illustrated by figure 3. Data are extracted from the RANS computation, then boundary layer turbulence is added as described in the previous section.

The grid sections in figure 2 give an overview of how the full domain was meshed for the eddy simulation. This is a structured, multi-block grid; the total number of computational blocks is 54.

Lengths are non-dimensionalized by the slot height, h, and velocities by the bulk velocity of the cooling jet, U_0. In these units, the nozzle lip thickness is 0.7. The surface between the lands slopes at about 3° from the horizontal. The origin is at the center of the breakout. The trailing edge is 8.3 slot heights from the breakout. The width of the breakout is 2. The overall domain width is 4.8. The Reynolds number based on the height and the bulk velocity of the channel is 7,385.

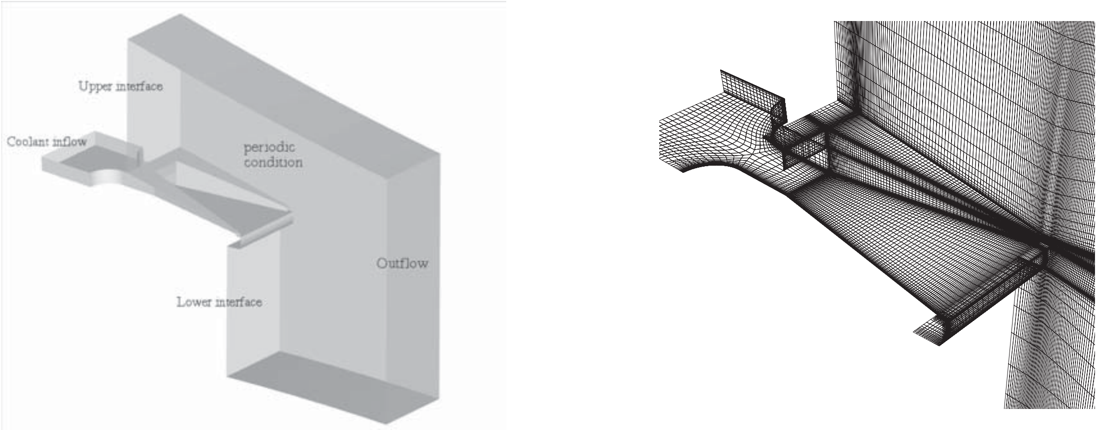

Figure 2: Schematic of the eddy simulation setup and sections of the grid.

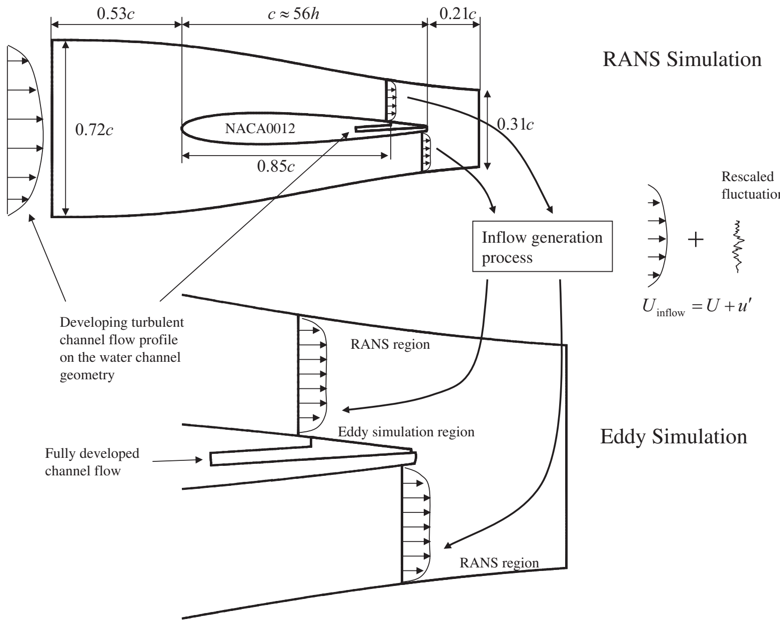

Figure 3: Schematic of the procedure of the trailing edge simulation.

Table 1: Grids refinement for the eddy simulations.

Case	Grid size near the slot	Total no. of comput. cells
Base	200x100x80	8.04×10^6
Final	224x152x128	20.0×10^6

Extensive grid refinement and validation studies are presented in Joo (2008). In a preliminary study, coarse grids with high stretching ratios caused severe grid-to-grid point oscillations and spurious, streamwise waves in the vorticity field. As a result of this preliminary study, a base grid was created with 8 million computational cells. The final grid was created by refining this in each of the x, y and z directions. Overall comparisons between the 8 million point grid and final grid resolutions are summarized in table 1. For the RANS simulations presented herein, a base grid of 2.47 million nodes was compared to a fine grid of 4.94 million nodes to verify grid independence (Joo, 2008).

Comparisons are illustrated by figure;a good number of similar comparisons were made by Joo (2008). Overall, the base and final cases are in good agreement, indicating that the final grid provides sufficient resolution.

RESULTS

Mean flow profiles at the two blowing ratios of $br = 1$ and $br = 1.5$ are provided in figure 4. These are shown at mid-span ($z = 0$). By $x = 3$ the profile has developed into a wall jet in a co-flowing stream. For the case of $br = 1$ the bulk velocity of the jet matches that of the free-stream and the profile develops the appearance of an accelerated boundary layer. For $br = 1.5$ the character of a wall jet in co-flow is present to the trailing edge. The eddy simulation and RANS profiles are quite similar except for the region around $x = 3$ where the secondary flows are captured in different quantities.

It turned out that SAS viscosity is less than three times the molecular viscosity in the breakout region. At the current Reynolds number, the full force of the hybrid RANS/eddy simulation character of SST-SAS is not coming into play. Rather the SAS model is functioning like an LES subgrid model.

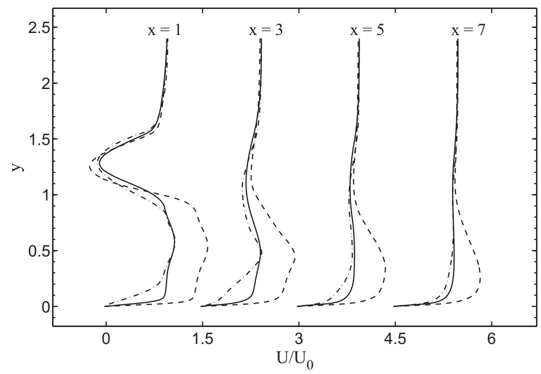

Figure 4: Mean velocity profiles in planes of constant z. ——: eddy simulation with br=1; - - -: eddy simulation with br=1.5; — · —: RANS with br=1.

More results and discussions are described at Joo and Durbin (2009).

Scalar mixing

Ultimately, we are concerned with turbulent mixing and heat transfer. Although we will refer to the 'temperature' field, a passive scalar was traced, rather than temperature, *per se*. This parallels the experimental practice of using CO_2 to study film effectiveness.

Improved predictions of film cooling effectiveness are presented in figure 5. The experimental data in these figures are for the geometry of Holloway et al. (2002a), which is similar to the present. The unsteady RANS simulation over predicts the adiabatic effectiveness.

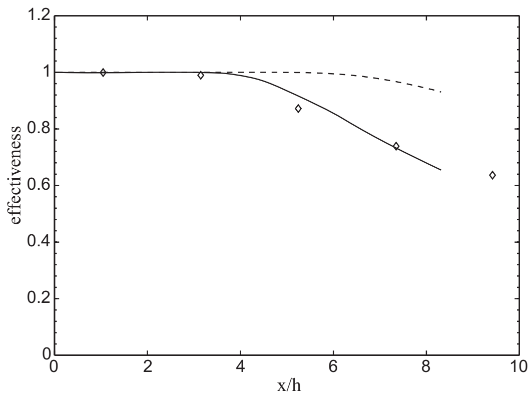

Figure 5: Film cooling effectiveness on the center line for br=1 ——: eddy simulation; - - -, RANS (Medic and Durbin, 2005); ◇, Experiment (Holloway et al., 2002a).

The ability of the eddy simulation to predict lower effectiveness indicates that the 'anomalous' mixing is being captured.

Sectional views of the SAS and RANS simulations are provided in figure 6. The cooling stream temperature is defined as 0 and the free stream temperature is normalized to 1. So temperature is contoured in these plots, with dark being the cool fluid and white the hot. The large scale undulations seen in the eddy simulation are suggestive of the ensemble average unsteadiness seen in the RANS result. The large scale, coherent unsteadiness has the same qualitative appearance. It seems that the qualitative features of mixing within the slot are captured by the RANS simulation. But *a discrepancy to the eddy simulation appears in the mixing just next to the lower wall*; it is the origin of incorrect cooling effectiveness.

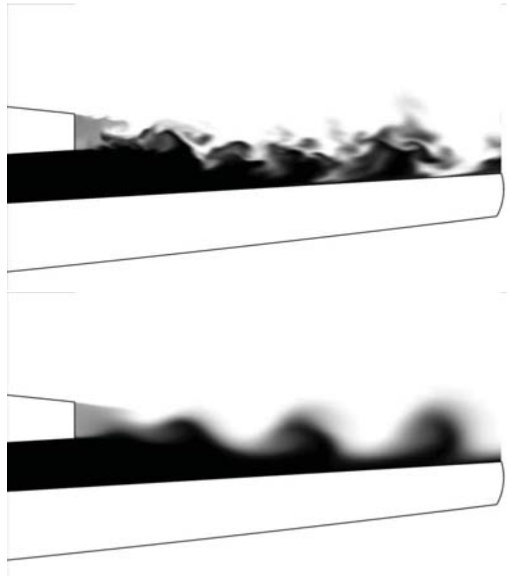

Figure 6: Instantaneous temperature contours at the center plane. Top: eddy simulation with br=1, bottom: RANS with br=1.

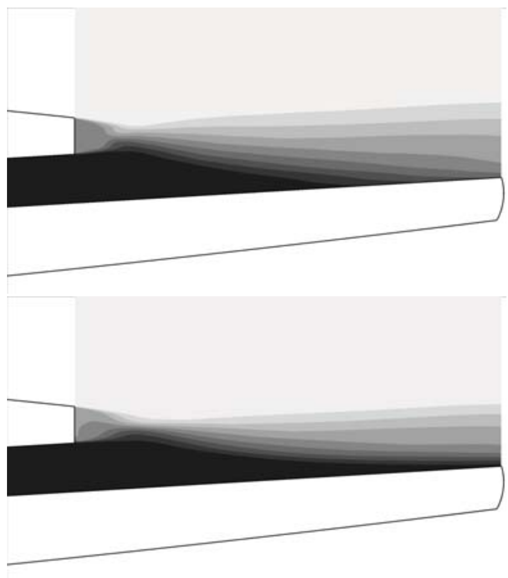

Figure 7: Mean temperature contours at the center plane. Top: eddy simulation with br=1, bottom: RANS with br=1.

The cooler layer next to the wall is disrupted by the large eddies in the eddy simulations, while the coherent vortex shedding does not carry hot fluid to the wall in the RANS computation. This may stem, in part, from transition in the initial separated shear layer. The RANS model assumes the layer is turbulent from the outset; in the eddy simulation the layer starts nearly laminar and becomes turbulent as three dimensional instabilities grow.

The time-averaged temperatures in figure 7 show the diffusion of the high, free-stream temperature toward the wall. The averaged effect of the eddies is to enhance diffusion; the dark region next to the wall is penetrated by gray contours in the left pane. In the lower pane the averaged effect of diffusion by Reynolds averaged vortices is too weak to mix the hotter fluid to the wall. Thus, it might be supposed that the turbulence model dissipates the vortices too strongly. It is probably more correct to say that it does not allow sufficient three-dimensionality to occur.

Spectra

Temporal energy spectra of velocity and temperature were calculated at selected locations within the slot. Representative spectra are presented in figure 8. These show a peak at the non-dimensional shedding frequency of 0.37 based on the height and the bulk velocity of the slot jet: fh/U_0. Recalling that the lip thickness above the slot is 0.7 times the slot height, the shedding Strouhal number is 0.26 when based on this thickness. The RANS simulation produced a Strouhal number of 0.24.

Velocity spectra at other locations were similar to those in figure 8 (Joo, 2008).

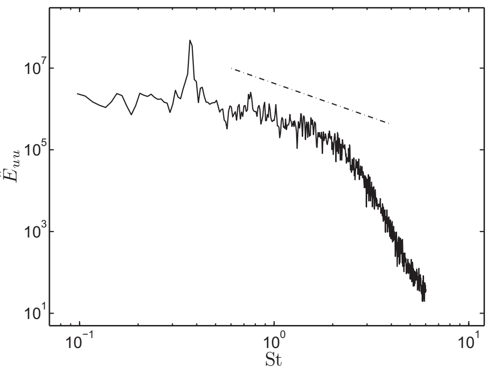

Figure 8: One dimensional streamwise energy in the center plane, at $x = 4$, $y = 0.571$ for the u spectrum. — · —: $k^{-5/3}$.

EDDY VERSUS UNSTEADY REYNOLDS AVERAGED SIMULATION

From a practical standpoint the question is whether anything can be concluded about why unsteady RANS does not predict the decline of film cooling effectiveness, η_{ad}. What property of the SST-SAS simulation leads to more correct behavior?

Although the unsteady RANS simulation over predicted film cooling effectiveness, the mean temperature profile shows that some degree of mixing occurred down to some point around $y = 0.5$. Figure 9 shows turbulent kinetic energy and mean temperature profiles in a plane at $z = 0.5$.

Around $y = 0.6$ the total kinetic energy of the RANS simulation — that is k, which is called the modeled kinetic energy in the figures, plus the time average of the mean fluctuation $1/2\langle(U(t) - \langle U\rangle)^2\rangle$, which is called the resolved kinetic energy of RANS — is of a level higher than the eddy simulation. At that height, the mean temperature also is comparable to or higher than eddy simulation. This shows there to be more mixing in the RANS simulation at those heights.

However, if we look closer to the lower wall, the total kinetic energy of the RANS simulation is significantly lower than seen in the eddy simulation; and so is the mean temperature. This indicates a strong correlation between the level of turbulent kinetic energy and the degree of mixing. Because η_{ad} is a measure of the wall temperature it is very directly related to mixing close to the surface. Below y of around 0.3 at $x = 4$, the resolved kinetic energy of RANS decreases sharply. This means that the resolved coherent motion does not penetrate below that height. *This would appear to be the primary factor in over predicting cooling efficiency.*

The turbulent kinetic energy of the eddy simulation is composed of around 35% large scale components, in the frequency band between zero and the shedding frequency (figure 8). The higher frequency components of turbulent kinetic energy in the eddy simulation correspond to the modeled turbulent kinetic energy, k, in the unsteady RANS simulation. Taken together, the set curves in figure 9 imply that the deficiency of *resolved eddying motion* relatively near to the wall is the biggest cause of deficient mixing in the RANS simulation. Thus one explanation of the anomalous mixing is that it arises from distortions of the coherent, shed vortices.

CONCLUSION

Unsteadiness in the trailing edge cooling slots consists of a coherent component and a broadband component. The coherent component is three dimensional vortex shedding. The eddy simulations discussed herein need not to distinguish the components. Indeed, they are not independent.

Both components are explicitly distinguished in unsteady RANS simulation: the coherent component appears as mean unsteadiness and the broadband component is represented by a closure model. They are coupled through turbulent kinetic energy production. Our primary conclusion is that the RANS representation is satisfactory above a layer next to the surface. Within that layer, RANS shows a suppression of mixing that does not occur in the eddy simulation. Evidence that the coherent motion is able to penetrate closer to the wall than predicted has been provided by the eddy simulation. Transition from laminar to turbulent flow after the trailing edge caused some additional difference between RANS and eddy simulations.

The dominant effect in this flow is three-dimensional vortex shedding caused by the upper nozzle lip. It has a profound influence on surface heat transfer because the lip is in proximity to the wall. These aspects of the geometry are essential to the fluid mechanics. We speculate that the particular lip thickness is not critical. However, our simulations offer a suggestion that any alteration to the nozzle lip that affects shedding might have a large effect on cooling. For instance distortion of the straight edge between the lands, or its junction with the lands could influence adiabatic effectiveness.

ACKNOWLEDGEMENT

This work was sponsored by the Airforce Office of Sponsored Research under grant, FA9550-05-1-0183 and by the Department of Energy Advanced Strategic Computing (ASC) program. We are grateful to Prof. J. K. Eaton for discussing the work with us.

REFERENCES

Barth, T., and Jespersen, D., 1989, "The design and application of upwind schemes on unstructured meshes", *AIAA Paper*, 89-0366.

Blaisdell, G., Spyropoulos, E., and Qin, J., 1996, "The effect of the formulation of nonlinear terms on aliasing errors

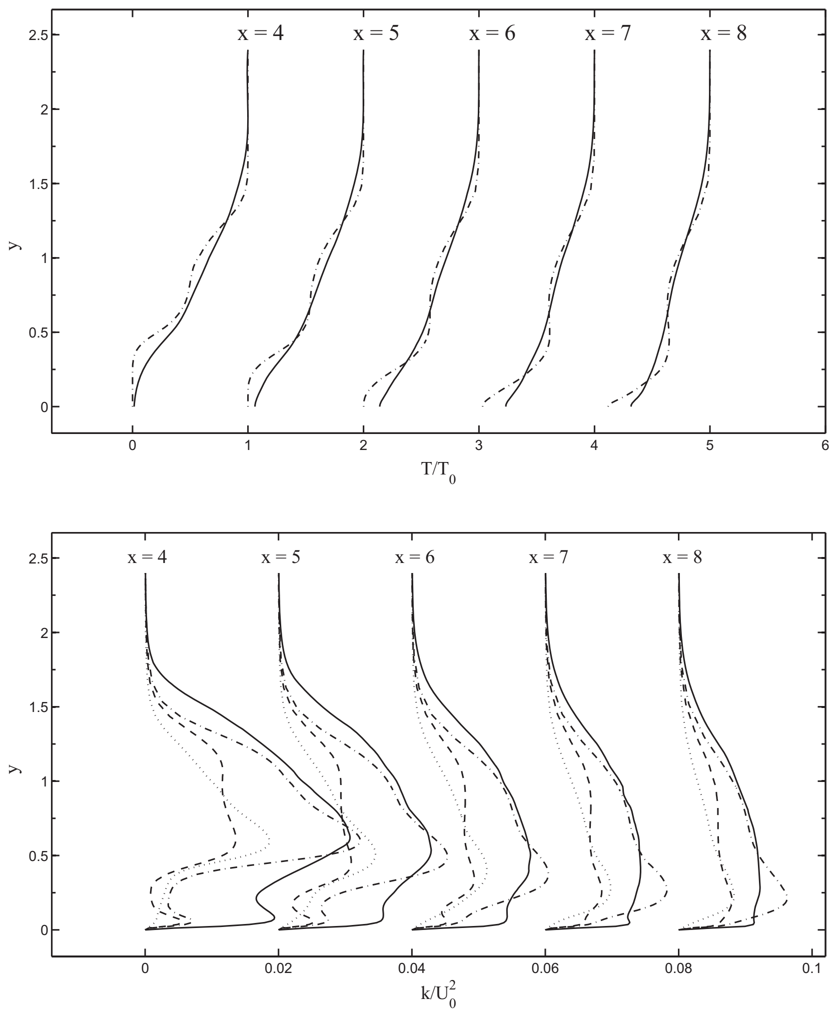

Figure 9: Comparison between turbulent kinetic energy and temperature mean profiles at z=0.5 plane with br=1. Top: mean temperature profiles; ——: eddy simulation; —·—RANS, bottom: turbulent kinetic energy; ——: eddy simulation; - - -modeled turbulent kinetic of RANS; ····resolved turbulent kinetic energy of RANS; —·—sum of the modeled and resolved turbulent kinetic energy of RANS.

in spectral methods", *Applied Numerical Mathematics*, Vol. 21, pp. 207-219.

Chen, Y., Matalanis, C. G., and Eaton, J. K., 2007, "High resolution PIV measurements around a model turbine blade trailing edge flim-cooling breakout.", *Experiments in-Fluids*, Vol. 44(2), pp. 199-209.

Holloway, S. D., Leylek, J. H., and Buck, F. A., 2002a, "Pressure-side bleed film cooling: part 1, steady framework for experimental and computational results", *ASME turbo expo 2002*, GT-2002-30471, pp. 835-843.

Holloway, S. D., Leylek, J. H., and Buck, F. A., 2002b, "Pressure-side bleed film cooling: part 2, unsteady framework for experimental and computational results", *ASME turbo expo 2002*, GT-2002-30472, pp. 845-853

Jameson, A., 1985, "Transonic flow calculations for aircraft, Lecture Notes in Mathematics", *Numerical Methods in Fluid Dynamics*, Vol. 1127, pp. 156-242.

Joo, J., 2008, *Eddy simulation of turbine blade trailing edge cooling*, Ph.D. thesis, Stanford University.

Joo, J. and Durbin. P. A., 2009, "Simulation of turbine blade trailing edge cooling", *Journal of Fluids Engineering*, Vol. 131, Issue 2, 021102

Kang, S., and Choi, H., 2002, "Suboptimal feedback control of turbulent flow over a backward-facing step", *Journal of Fluid Mechanics*, Vol. 463, pp. 201–227.

Lele, S. K., 1992, "Compact finite difference schemes with spectral-like resolution", *Journal of Computational Physics*, Vol. 103, pp. 16-42.

Lund, T. S., Wu, X., and Squires, K. D., 1998, "Generation of turbulent inflow data for spatially-developing boundary layer simulation", *Journal of Computational Physics*, Vol. 140, 1998, pp. 233-258.

Medic, G., and Durbin, P. A., 2005, "Unsteady effects on trailing edge cooling", *ASME Journal of Heat Transfer*, Vol. 127, pp. 388-392.

Menter, F. R., 1992, "Two-equation eddy-viscosity turbulence models for engineering applications", *AIAA Journal*, Vol. 32, pp. 1598-1605.

Menter, F. R., and Egorov, Y., 2005a, "A Scale-adaptive simulation modeling using two-equation models", *AIAA Paper*, 2005-1095.

Menter, F. R., and Egorov, Y., 2005b. "Self-adaptive simulation of aerodynamic flows", Tech. rep., ANSYS.

Van der Weide, E., Kalitzin, G., Schlüter, J., and Alonso, J., 2006 "Unsteady turbomachinery computations using massively parallel platforms", *AIAA Paper*, 2006-421.